Accepted Manuscript

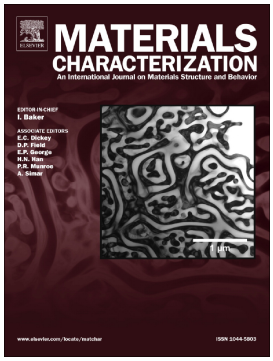

Evaluation of the influence of texture and microstructure of titanium substrates on TiO2 anodic coatings at 60V

María Laura Vera, Martina Cecilia Avalos, Mario Roberto Rosenberger, Raúl Eduardo Bolmaro, Carlos Enrique Schvezov, Alicia Esther Ares

PII: S1044-5803(16)31306-7
DOI: doi: 10.1016/j.matchar.2017.07.005
Reference: MTL 8742

To appear in: *Materials Characterization*

Received date: 28 December 2016
Revised date: 6 June 2017
Accepted date: 1 July 2017

Please cite this article as: María Laura Vera, Martina Cecilia Avalos, Mario Roberto Rosenberger, Raúl Eduardo Bolmaro, Carlos Enrique Schvezov, Alicia Esther Ares , Evaluation of the influence of texture and microstructure of titanium substrates on TiO2 anodic coatings at 60V, *Materials Characterization* (2017), doi: 10.1016/j.matchar.2017.07.005

Evaluation of the influence of texture and microstructure of titanium substrates on TiO_2 anodic coatings at 60 V

María Laura Vera[a,*], Martina Cecilia Avalos[b], Mario Roberto Rosenberger[a], Raúl Eduardo Bolmaro[b], Carlos Enrique Schvezov[a], Alicia Esther Ares[a]

[a]Instituto de Materiales de Misiones (IMAM), CONICET-UNaM. Félix de Azara 1552 (3300) Posadas, Misiones, Argentina

[b]Instituto de Física Rosario (IFIR), CONICET-UNR. Electron Microscopy Laboratory, CCT Rosario. Bvrd. 27 de Febrero 210 bis (2000), Rosario, Argentina

ABSTRACT

The current paper analyzes the influence of texture and microstructure of Ti substrates on morphology and color of titanium dioxide coatings obtained by anodic oxidation. Substrates of Ti grade 2 and Ti grade 5 with different thermo-mechanical histories were used in the shape of cylindrical bars cut in both longitudinal and transversal directions, and laminated sheets. The crystalline orientation of the surface grains in the substrate before oxidation, were determined by electron backscatter diffraction. The oxide coatings were analyzed by optical and scanning electron microscopy. The results show that different substrate grain orientations produce oxides with different colors, because of different thickness depending on their orientations. An oxide grown on a basal hcp plane, with higher atomic density is thinner than an oxide grown on a transversal hcp plane with lower atomic density. This effect is more pronounced on elongated grains. Different anodic oxidation process parameters and heat treatments of the substrate were applied in order to

* Corresponding author; e-mail: lauravera@fceqyn.unam.edu.ar; veramalau@gmail.com.ar; phone: +54-0 376-4497141; fax: 54 11 6772 7886.

obtain a more uniform oxide thickness. A specific heat treatment of the substrate was the most efficient, starting from a favorable orientation of crystals, characteristic of rolling texture.

Keywords: TiO_2 anodic coatings, 60 V, EBSD, colors oxide, texture

1. Introduction

Anodic oxidation is a simple and low cost electrochemical technique to obtain oxide coatings over metallic substrates [1,2]. The characteristics and properties of the coatings depend on the electrochemical parameters (voltage, current density, electrolyte, etc) applied in the oxidation [1,2,3,4].

Titanium dioxide synthetized by anodic oxidation is widely investigated due to its interesting applications roughly divided into energy, environmental [5], biomedical [6] and esthetic [7] categories.

In the literature it is reported that TiO_2 coatings obtained by anodic oxidation on laminated Ti-6Al-4V present a color pattern composed of one predominant color with small portions of other different colors, quasi-homogeneously distributed on the surface [8,9,10] with some hue and shade variations, which remains also after heat treatments performed after anodic oxidation [9,11].

With most electrolytes, the color of the anodic TiO_2 coating obtained at low voltages is directly related to its thickness [10,12], and consistently resulted in only one global value of measured thickness [8,9,10]. However, in anodic coatings obtained on sheets of Ti-6Al-4V with sulfuric acid as electrolyte and an applied voltage of 60 V, Vera et al. [8,9] observed a color contrast larger than in thinner coatings obtained at lower voltages. Two different colors (yellow and pink) were observed, indicating regions of coatings with different thicknesses. In fact, in those samples two values of thickness were determined and associated to each color [9].

It was reported that different thicknesses in coatings on commercially pure (cp) Titanium were obtained by anodic oxidation for different crystal orientations of the substrate grains [13,14,15,16,17,18]. Accordingly, it was proposed that the different colors in TiO_2 coatings on laminated Ti-6Al-4V could be due to different crystal orientations of the substrate grains influencing the coating thickness.

For investigating this proposition, the crystal orientations of the grains of Ti-6Al-4V plates used as substrates were determined, and the relation with the color of the coating was analyzed. The grain crystallographic orientations were determined by electron backscatter diffraction (EBSD).

In the present report, coatings obtained by anodic oxidation with a 1 M sulfuric acid electrolyte at 60 V were analyzed. The influence of grain orientation, or texture, for both types of samples, cp Ti and Ti-6Al-4V alloy plates, is presented, and the correlation with the anodic coating thickness is analyzed. Finally, options to eliminate the bi-color effect are suggested.

2. Materials and methods

2.1. Substrate preparation

Commercially pure (cp) Ti (99.5 wt %) and Ti-6Al-4V alloys, known as Ti grade 2 and 5 respectively (ASTM B 367 [19]), were employed as substrates. They are referred as TiG2 and TiG5 samples respectively.

Two forms of TiG5 were used; a circular bar (30 mm in diameter) and a plate (2 mm thick). The TiG2 was used only in plate form. To obtain samples of the cross section bar, it was cut in the cross section as cylindrical discs, 3 mm thick, which were then divided into 4 equal portions as quadrants, approximately 5 cm^2 of total surface area. In addition, longitudinal samples of the bar were obtained by cutting pieces parallel to the axis of the bar, as shown in the diagram of Figure 1. Rectangular samples (10 x 20 mm^2) were cut from the plates of TiG2 and TiG5 (Figure 1). The substrate surfaces were prepared for oxidation as follows.

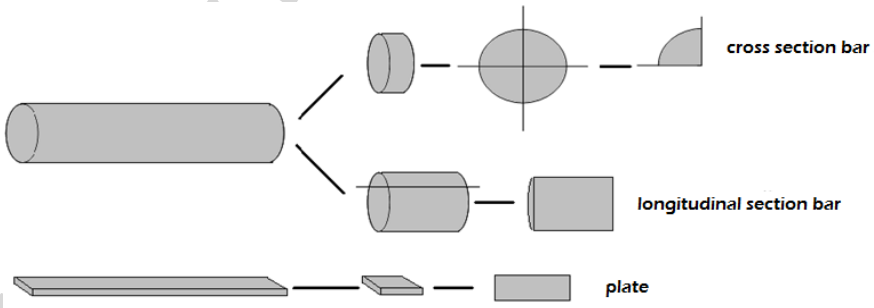

Figure 1. Scheme of the different geometries of samples used. Round bar sample was only of the TiG5 variety. Plates were for TiG5 and TiG2 alloy varieties.

The substrates were mechanically polished with SiC abrasive papers of sizes ranging from #240 up to #1500, and then polished, first with 1 μm diamond paste lubricated with ethylene glycol and then with a 4:1 mixture of colloidal silica (Mastermet 2 and hydrogen peroxide, H_2O_2 20% v/v) on a soft

cloth. The mirror-finished surfaces were then washed with detergent and water, rinsed with ethyl alcohol and dried with hot air.

To reveal the microstructure of the substrates without coating, the Ti alloys were etched with a Kroll solution of composition: 5% HF, 30% HNO_3 and 65% H_2O for 1 s.

For the EBSD measurements, the polishing strategy consisted in using 400 through 2000 grit polishing paper followed by 9, 6, 3 and 1 µm diamond paste on polishing cloth and further vibratory polishing with colloidal silica.

2.2. Determination of the substrate crystallographic orientation

For determining the individual crystal orientations of the grains of the TiG2 and TiG5 alloys used as substrates, the EBSD technique was employed using a field emission scanning electron microscope (FE-SEM) FEI Quanta 200F equipped with a TSL OIM EBSD system. Image quality (IQ) maps constructed from EBSD data provide useful visualizations of microstructure. Inverse Pole Figure (IPF) maps can illustrate the crystal direction perpendicular to the sample surface of each grain.

Other texture measurements were directly performed by X-ray methods in a Panalytical X-Pert Pro MPD equipment. The diffractometer is suited with and Eulerian cradle, Cu Kα radiation, X-ray lens and Xe detector. Five incomplete pole figures were measured and corrected for defocusing and background. Recalculated pole figures and inverse pole figures were obtained through the calculation of Orientation Distribution Functions by using wxpopLA, the current Windows XP version of the popLA package [20].

In order to correlate crystal grain orientations of the substrates with coating thicknesses, each sample of TiG2 and TiG5 plates were indented in several zones for reference, as shown in Figures 2 and 3, respectively. IPF images were taken from each reference zone before anodic oxidation.

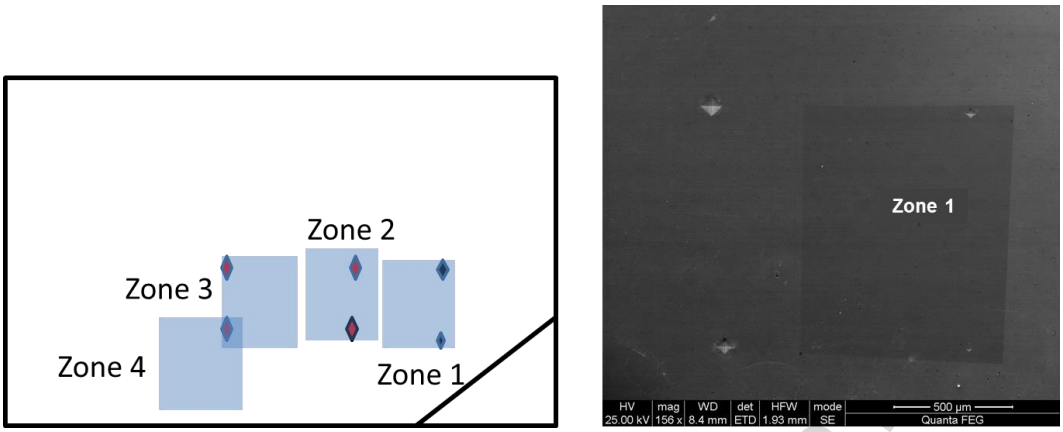

Figure 2. Diagram of the marked zones of the TiG2 plate to be examined by EBSD before anodic oxidation.

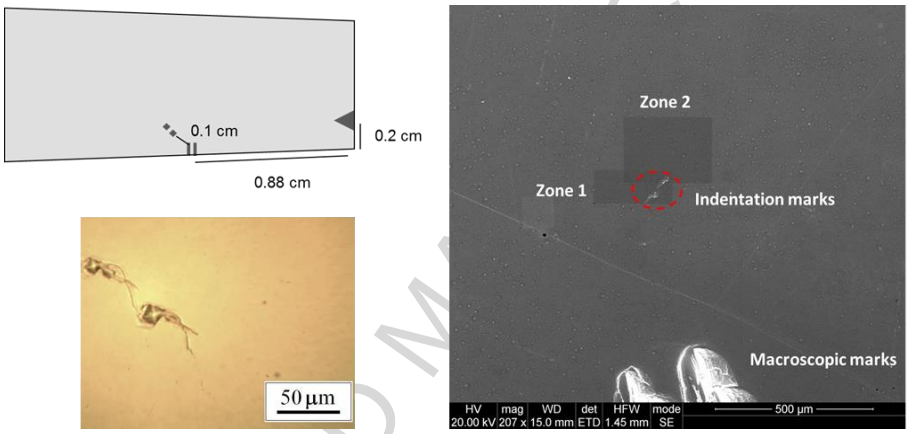

Figure 3. Diagram of the marked zones of the TiG5 plate to be examined by EBSD before anodic oxidation.

2.3. Anodic oxidation

The samples were anodically oxidized at 60 V for 1 min in a 1 M H_2SO_4 electrolyte solution. The mirror like polished Ti alloy substrate was used as anode and a Pt wire as cathode at a distance of 5 cm from the anode. A volume of 150 ml of the electrolyte is used and oxidation is performed at room temperature. The applied voltage reached 60 V by steadily increasing from 0 at a constant rate of 1.2 V/s, and remained constant in a potentiostatic mode during 1 min. After oxidation, the sample is withdrawn, rinsed with demineralized water and dried with hot air.

Color observations were made with an optical microscope (Arcano) where the sample was illuminated with an incandescent light with a predominant yellow spectrum (additional data of spectrum are provided in the Supporting Information, SI, section S1). All micrographs were taken under the same conditions of illumination, because it is extremely important to standardize the

illumination to be able to compare the effects in the color, especially when the changes are very subtle. Micrographs of color coatings were analyzed using the Wolfram Mathematica software (version 8) [9].

2.4. Options to promote a reduction on oxide film thickness dispersion

2.4.1. Anodic oxidation process parameters

The optimum oxidation parameters should reduce the variations in oxide thickness from grain to grain to obtain a smooth coating thickness in the entire sample. In search of the optimum process, some of the oxidation parameters described in Section 2.3 were varied as shown in Table 1. Every oxidation was performed at 60 V with 1 M H_2SO_4 electrolyte.

Table 1. Oxidation parameters used to reduce variations in oxide thickness from grain to grain of the substrate*.

Options	Rate of voltage increase [V/s]	Oxidation time [min]	Electrolyte stirring	Electrolyte temperature [ºC]
Base	1.2	1	no	25
A	**5.8**	1	no	25
B	5.8	**15**	no	25
C	5.8	1	**yes**	25
D	5.8	1	no	**40**
E	5.8	**10**	no	**40**

* The values of the parameters varied in each case are highlighted in **bold** letters.

TiG5 substrate without coating and samples oxidized at different electrolyte temperatures and during different time lapses (B, D and E) were analyzed by X-ray diffraction using a Philips PW 3710 diffractometer with CuKα wavelength, using a thin-film Philips device that allows operation with a glancing incidence angle of 1°.

2.4.2. Heat treatment of substrates

Before anodic oxidation, samples of TiG5 plates were heat treated, in order to modify the texture and microstructure, as shown in Table 2.

These samples, after heat treatment, were mirror polished as described in Section 2.1, their structures were determined and they were anodically oxidized at 60 V for 1 min with a 1 M H_2SO_4 solution at 25 ºC, using a rate of 5.8 V/s and no stirring.

Table 2. Heat treatments of plate TiG5 substrates to reduce variations in oxide thickness from grain to grain of the substrate.

Options	Temperature [ºC]	Time [h]	Cooling to ambient temperature
TT1	850	1	Slow inside the furnace
TT2	850	3	Slow inside the furnace
TT3	950	4	At 1 ºC/min to 760 ºC and then air cooled

3. Results and discussion

3.1. Coatings produced on TiG5 and TiG2

The microstructures of the TiG5 substrates before oxidation are shown in Figure 4. The microstructure depends on the type of sample (described previously in Figure 1). Figure 4 (a) shows the microstructure of a cross section of a TiG5 bar presenting a structure of α equiaxed grains surrounded by β grains. Figure 4 (b) shows the microstructure of the longitudinal section of the TiG5 bar in the axial direction with elongated α grain widths of 12 μm approximately. In Figure 4 (c) the TiG5 plate shows an elongated grain structure similar to that observed in Figure 4 (b), but with thinner α grains. The structures are consistent with the hot lamination process at 900 ºC used in the production of both materials; the bar and the plate. The effect of lamination can be noted comparing the cross section with the longitudinal section of the bar shown in Figures 4 (a) and (b), respectively; the first showing a nearly equiaxed grain structure and the second an elongated grain structure.

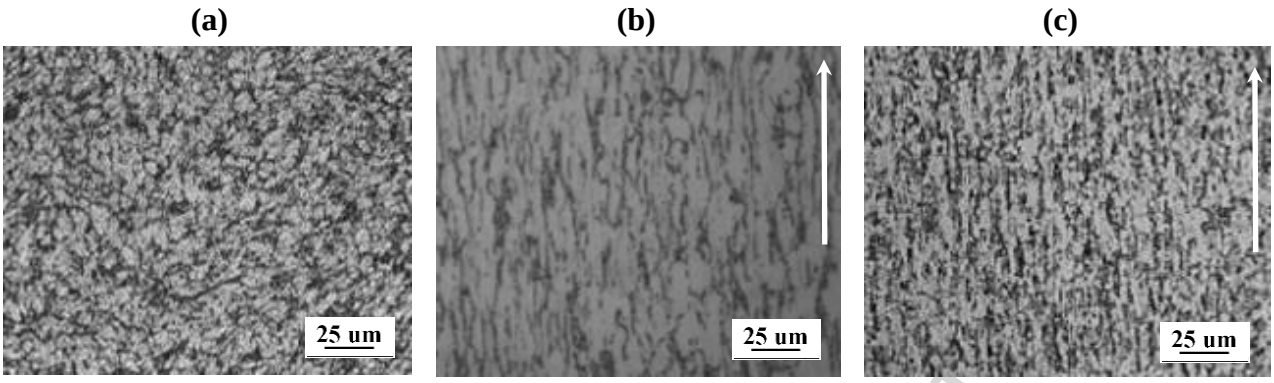

Figure 4. Optical micrographs of the microstructure of TiG5 substrates: (a) cross section of the bar; (b) longitudinal section of the bar; (c) plate. The white arrow indicates the lamination direction.

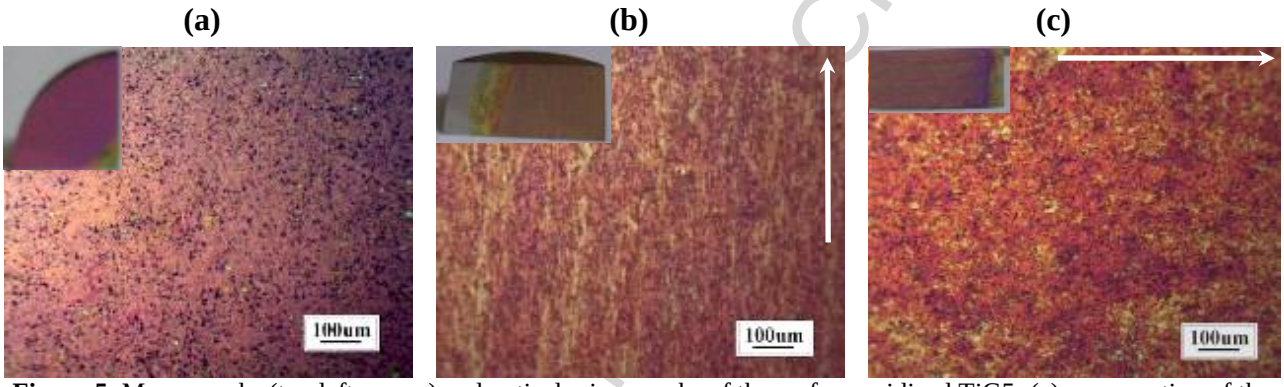

Figure 5. Macrographs (top left corner) and optical micrographs of the surface oxidized TiG5: (a) cross section of the bar; (b) longitudinal section of the bar; (c) plate. The white arrow indicates the lamination direction.

Samples with the structure shown in Figure 4 were anodically oxidized in a 1 M H_2SO_4 solution at 60 V for 1 min without stirring; the resulting coating surfaces are shown in Figure 5.

The coating obtained in a cross section of the bar with an equiaxed structure is shown in Figure 5 (a); the TiO_2 coating color is pink with some different hues and interspersed dark points. The dark points correspond to pores of the coating, which were confirmed by SEM observations. In addition, in Figure 5 (a) some small and dispersed zones show a yellow color, associated with β phase interspersed between the majority of α grains, as is shown in the Figure S2 of SI, section S2. In the case of the coating produced on a longitudinal section of the bar the result is as shown in Figure 5 (b). In this Figure, the colors of the coating are yellow and pink following the elongated grains of the substrate microstructure. In Figure 5 (c), corresponding to the coating produced on TiG5 plate, similar patterns of pink and yellow, corresponding to an elongated structure as in Figure 5 (b), are observed.

Comparing Figures 4 and 5, it is noted that the difference in color, pink or yellow, is more pronounced in Figures 5 (b) and (c), with substrates presenting larger and elongated α grains as shown in Figures 4 (b) and (c). ~~The color of the coating shown in Figure 5 (a) is more uniform for a substrate with a microstructure presenting smaller and equiaxed grains (Figure 4 (a)).~~

In the case of a TiG2 in plate form, the structure of the substrate before oxidation is shown in Figure 6 (a) and the coating after oxidation in Figure 6 (b). The color of the coating is yellow with a few regions with a hue of the same color.

These results show that the texture of the substrate has an important effect on the different thickness of the coating produced by anodic oxidation. In the following sections, the texture of the substrate is determined and the color of the coating is analyzed.

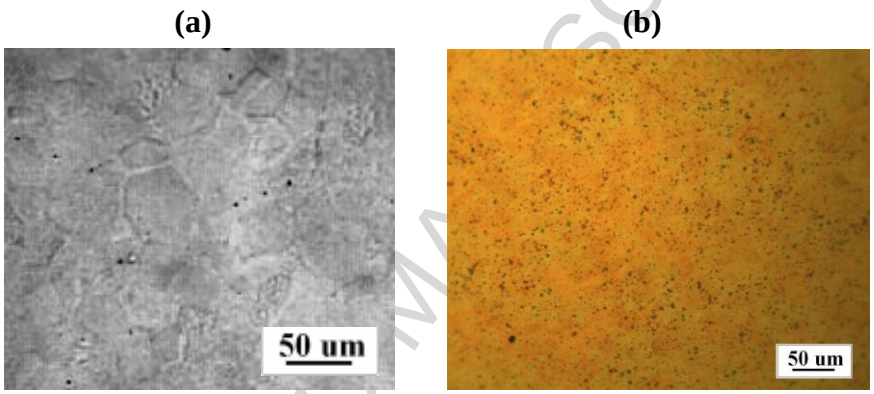

Figure 6. Optical micrographs of: (a) microstructure of TiG2 plate; (b) anodic coating on TiG2 plate.

3.2. Characterization of grain directions and oxide film color on TiG2 plate

Representative EBSD scans for the substrate of the TiG2 alloy are shown in Figures 7. The scans were indexed assuming the presence of α phase (hcp). The average grain size of the sample is 35 ± 20 μm and the texture is typical of cold rolled Ti [21] with basal poles tilted $\pm 20^0$-40^0 away from the normal direction against the transverse direction, as it is evident from Figure 8 (a).

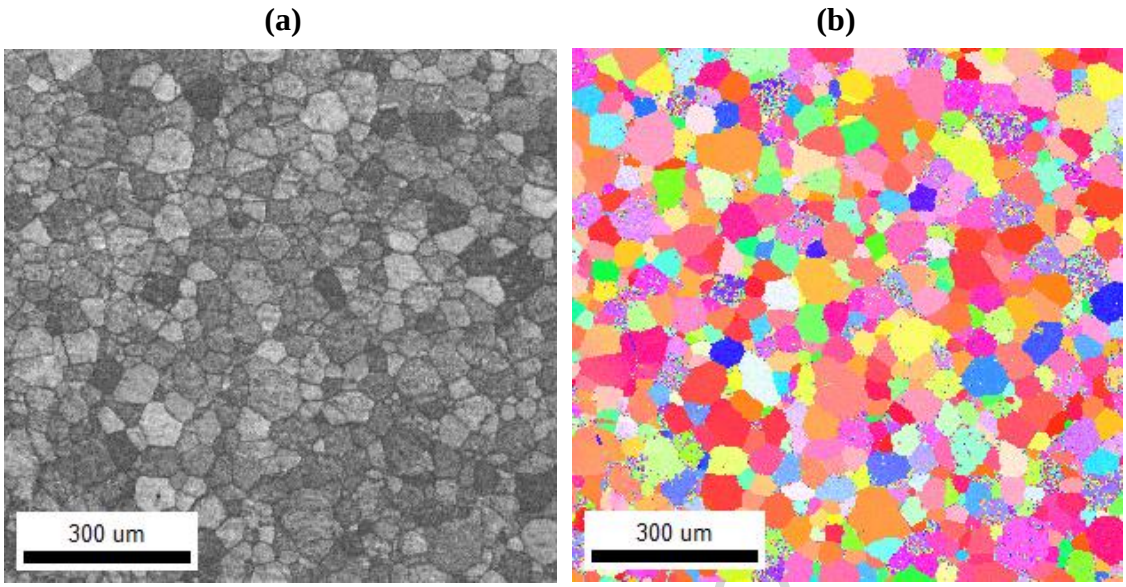

Figure 7. EBSD images of Zone 1 of the TiG2 plate: (a) microstructure of the α grains shown by the IQ map; (b) IPF image.

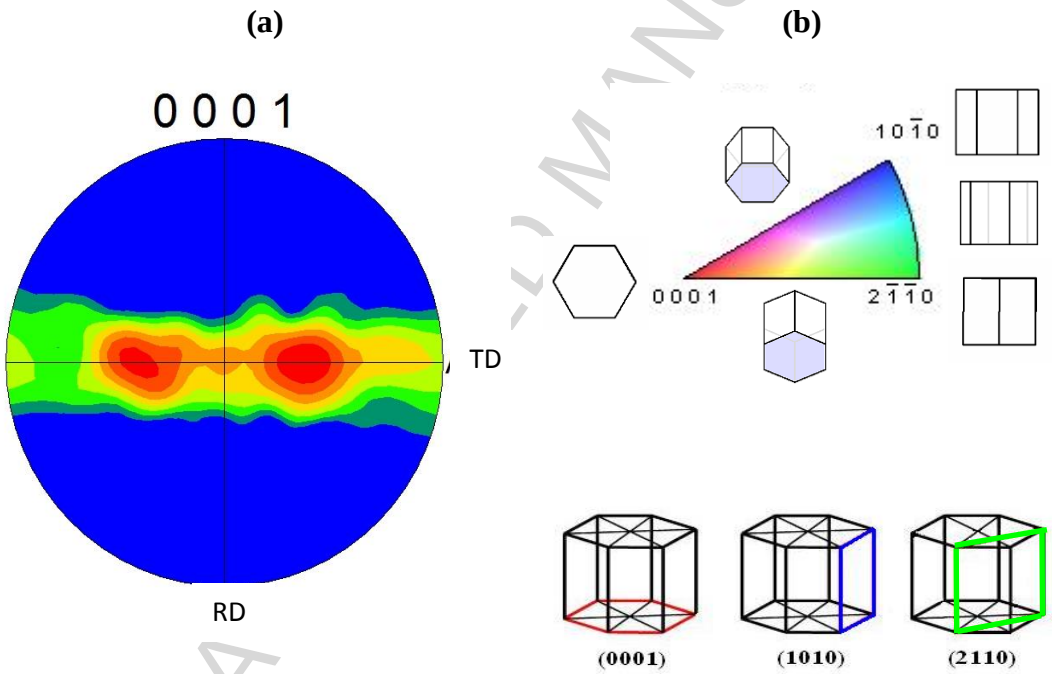

Figure 8. (a) (0001) pole figure of the TiG2 plate samples; (b) color code scale on the IPF images of the α (hcp) phase depending on the corresponding crystal directions perpendicular to sample surface; and scheme of characteristic planes in the hcp structure. RD: rolling direction; TD: transversal direction. Adapted from [21].

Once the texture of the TiG2 plate was determined, it was anodically oxidized using a 1 M H_2SO_4 solution at 60 V for 1 min. The EBSD maps and the optical micrographs are shown in Figure 9 (a) and 9 (b) for Zones 1 and 2.

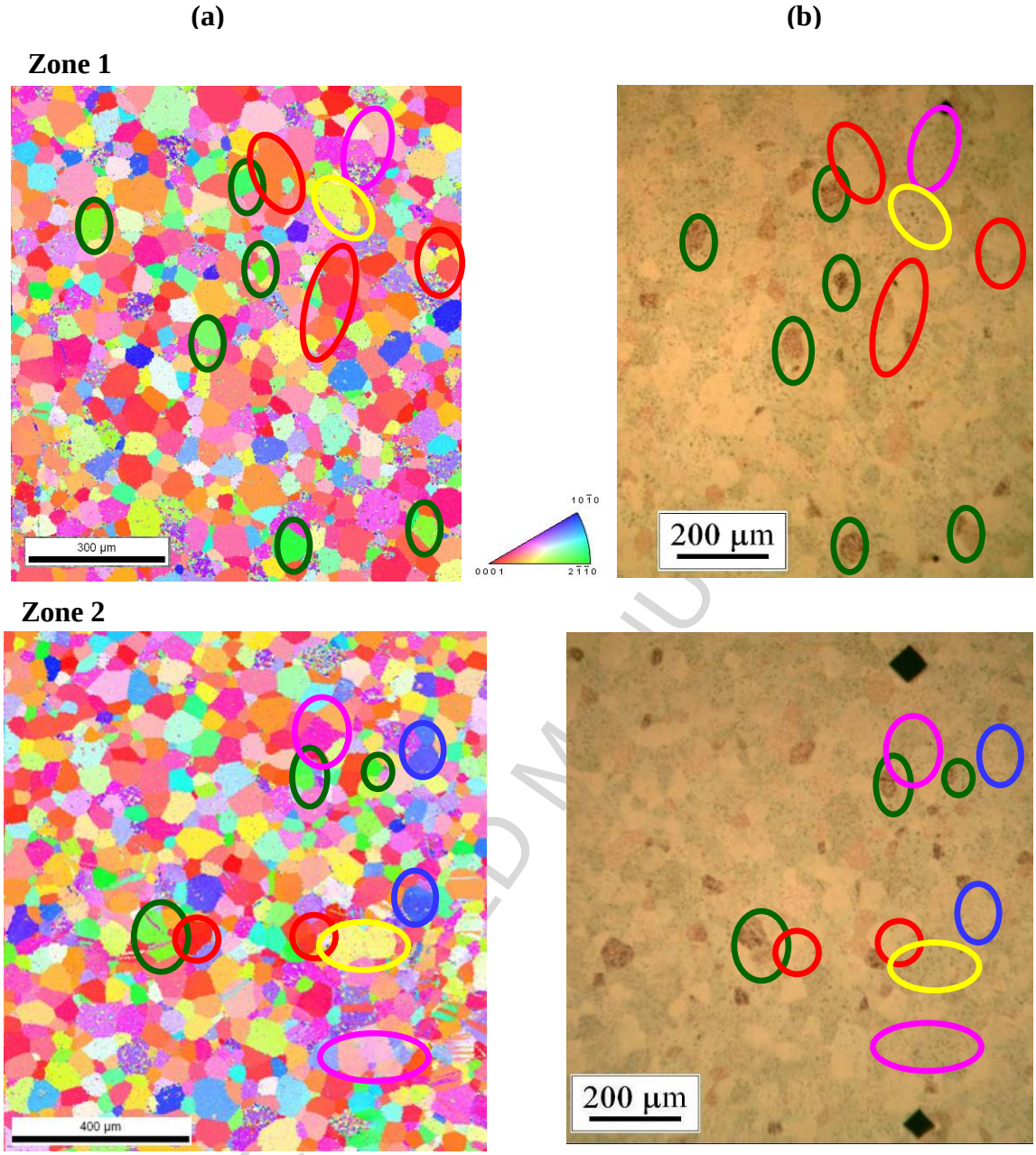

Figure 9. Comparison between: (a) IPF images of Zones 1 and 2; (b) Optical micrographs of anodic coatings of Zones 1 and 2. The color of the coating depends on orientation, as shown in the next examples: grains oriented with basal planes parallel to the surface show a homogeneous yellow color after oxidation (red ovals, (0001)). The oxide grown in grains with $(2\bar{1}\bar{1}0)$ planes parallel to surface sample have a dark yellow-orange color (green ovals). The grains pointing up at around 45º from basal plane acquire a yellow-green film after oxidation (e.g. pink ovals, $(11\bar{2}0)$ and yellow ovals). Blue ovals surround grains pointing up with the $(10\bar{1}0)$ direction.

To analyze the influence of the grain orientation on the growth characteristics of oxide film, the normal direction inverse pole figure can provide information on the crystal direction aligned with

the normal to the surface of the substrate. For comparison with the anodized surfaces, the corresponding IPF images extracted from EBSD results, filtered by directions perpendicular to ND, are shown for the same zones before oxidation in Figures 10. The relative area for the main group of directions in IPF images, the corresponding film color after oxidation and an approximate correspondence with crystalline texture components are also shown.

Orientation	(0001)<uvtw>	(10$\bar{1}$0)<uvtw>	(hkiℓ)<uvtw> with ~ 10 < ℓ < 25	(2$\bar{1}\bar{1}$0)<uvtw>
ND IPF	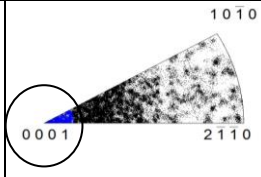	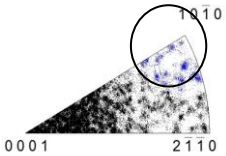	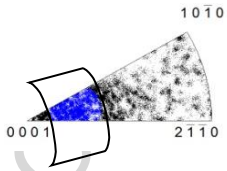	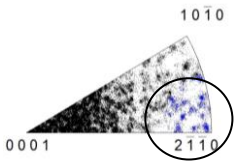
Volume fraction	15%	7%	40%	7%
Oxide film color	yellow	yellow	yellow-green	yellow-orange
EBSD filtered results of Zone 1 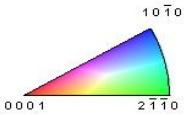	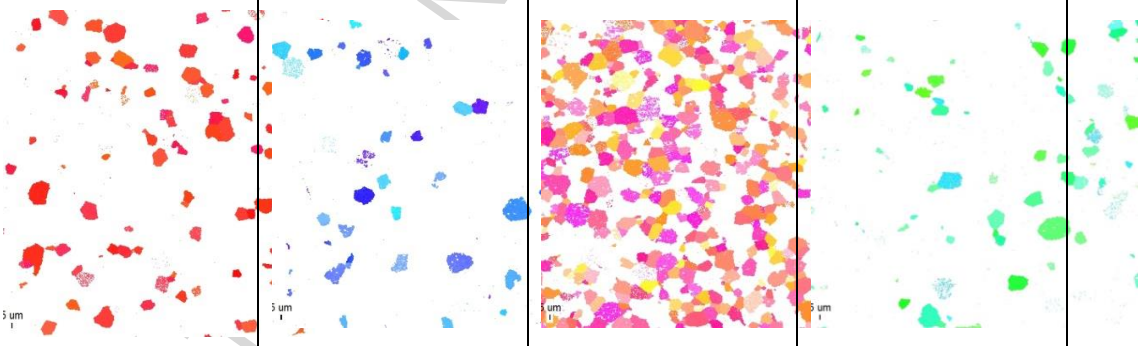			
EBSD filtered results of Zone 2 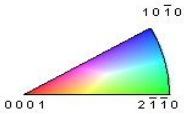	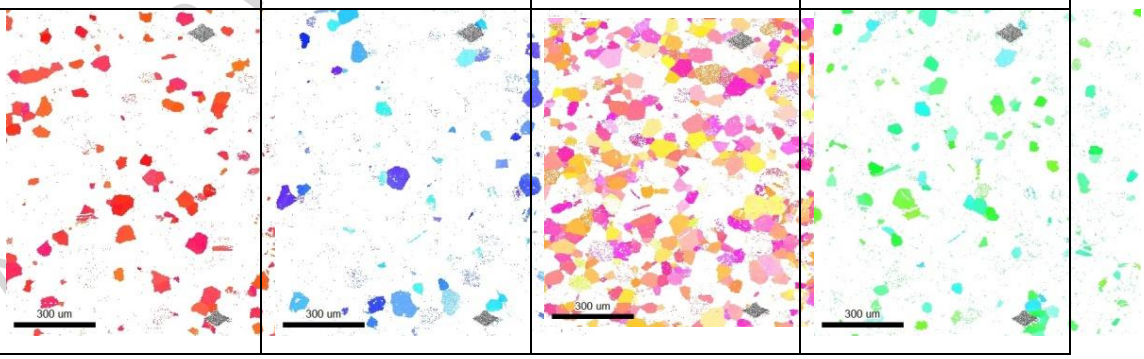			

Figure 10. ND IPF. Texture components approximately separating crystals by surface colors. Mean area (%) of TiG2 samples with different directions and the corresponding oxide color after anodizing. 41% of the area corresponded to other orientations. Circles surround crystal direction components.

3.3. Characterization of grain directions and oxide film color on TiG5 plate

The same procedure as in TiG2 plate (Section 3.2) was applied in the case of TiG5 plate to analyze the relation between crystal grain orientation and the corresponding color of the oxide film formed in each grain. The analysis, however, is more complex than in the case of the TiG2 plate since the grain structure of the substrate is different, in size and phases. The microstructure of TiG5 plate consists of a majority of α phase (98%) and a 2% of β phase, grains of around 1 μm size interspersed between the majoritarian α grains.

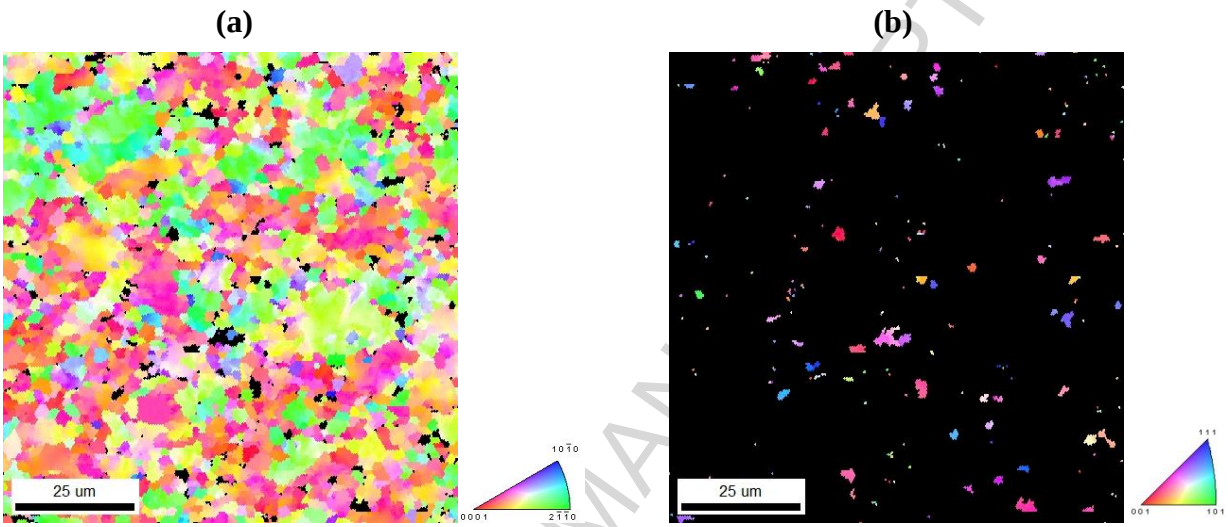

Figure 11. (a) IPF of TIG5 α phase; (b) IPF of TIG5 β phase.

Figures 11 (a) and (b) show representative IPF maps of α and β phases, which are easily separated by EBSD by making two partitions. In each of these maps, the absent phase is in black. Figure 12 (a) correspond to an IQ map of a TiG5 plate. The average grain size is 3 ± 2 μm for α phase and 1.5 ± 0.5 μm for β phase. The ED//(001) (in the specimen system) inverse pole figure of the sample indicates a texture compatible with a hot hydrostatic extrusion as it is evident in Figure 12 (b). The results shown here are in agreement with the texture reported for below 900 ºC hot laminated Ti-6Al-4V alloys [22,23,24].

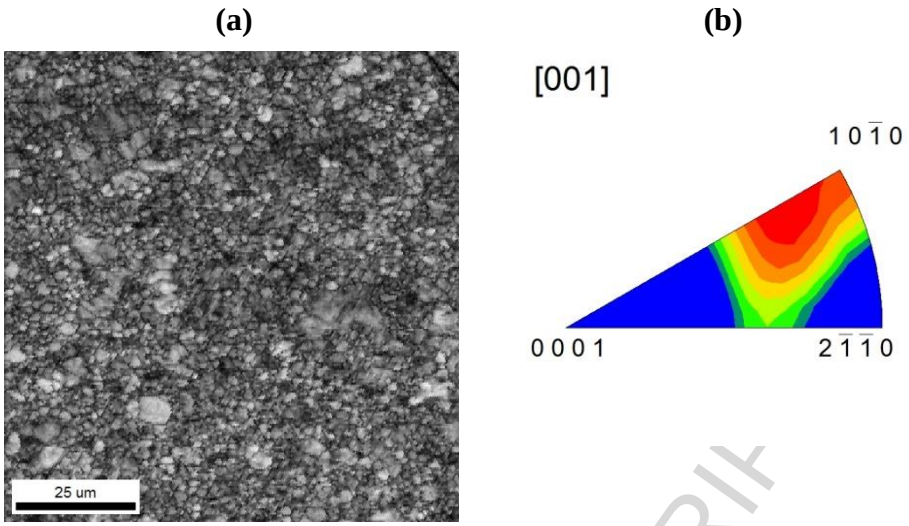

Figure 12. (a) IQ map of TiG5 sample; (b) ED-[001] direction IPF of the TiG5 samples.

As it was mentioned for TiG2 sample, the normal direction inverse pole figure was used to analyze the influence of the grain orientation on the growing oxide film. The relative area for the main group of directions in IPF images and the corresponding film color after oxidation are listed in Figure 13.

Figures 14 (a) show islands of fine grains pointing perpendicularly out of the surfaces following a fiber on the IPF diagram from the (0001) direction (red grains on EBSD IPF color convention) up to the $(2\bar{1}\bar{1}0)$ direction (green grains on EBSD IPF color convention), passing through $(10\bar{1}3)$ and $(11\bar{2}4)$.

The relation between substrate grain directions given by the IPF image and the resulting coating can be seen in Figure 14 (b) showing the micrograph of the oxide film. It is yellow for (0001) basal and $(10\bar{1}3)$ directions, the last one highly populated as a consequence of the hot rolling process, and pink for each $(11\bar{2}4)$, $(2\bar{1}\bar{1}0)$ and $(10\bar{1}0)$. The other directions in IPF images have not been specifically correlated to oxide film colors; however, the oxides are also yellow and pink. According to Figure 14 (b), approximately 55% of the surface area of oxide film is pink, 34% is yellow and 10% has other colors or is black.

Orientation	(0001)<uvtw>	(10$\bar{1}$0)<uvtw>	(10$\bar{1}$3)<uvtw>	(11$\bar{2}$4)<uvtw>	(2$\bar{1}\bar{1}$0)<uvtw>
ND IPF 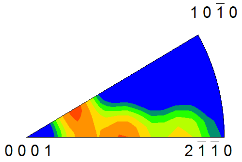	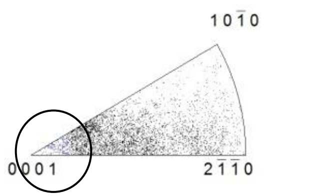	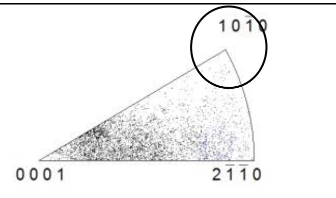	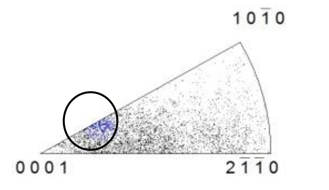	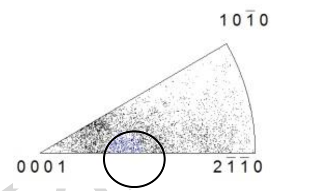	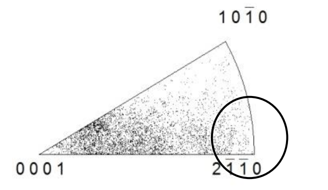
Volume fraction	5%	5%	16%	15%	13%
Oxide film color	Yellow	Pink	Yellow	Pink	pink
EBSD filtered results 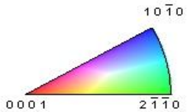	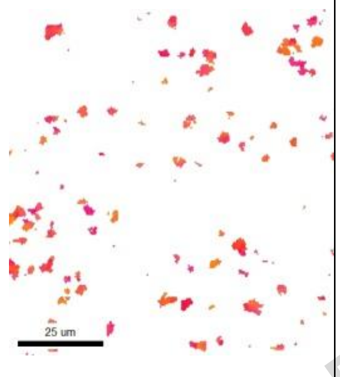	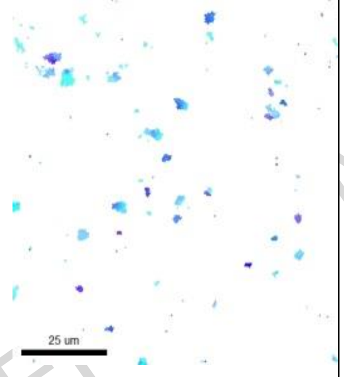	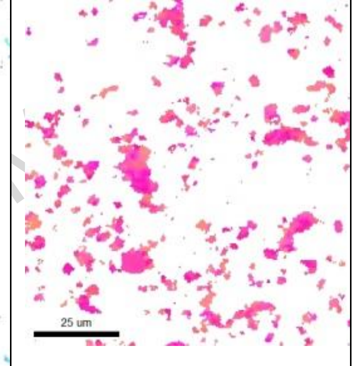	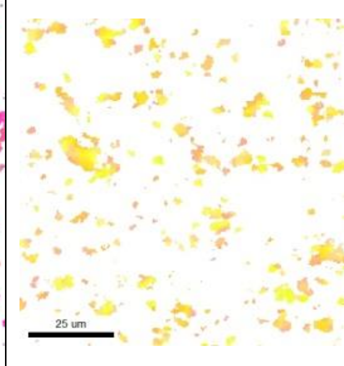	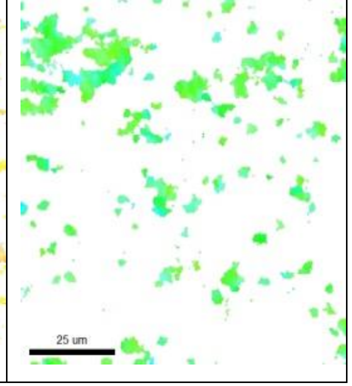

Figure 13. ND IPF for TiG5 plates. Texture components approximately separating crystals by surface colors. Mean area (%) of TiG5 samples with different directions and the corresponding oxide color after anodizing. 46% of the area corresponded to other directions. Circles surround crystal direction components.

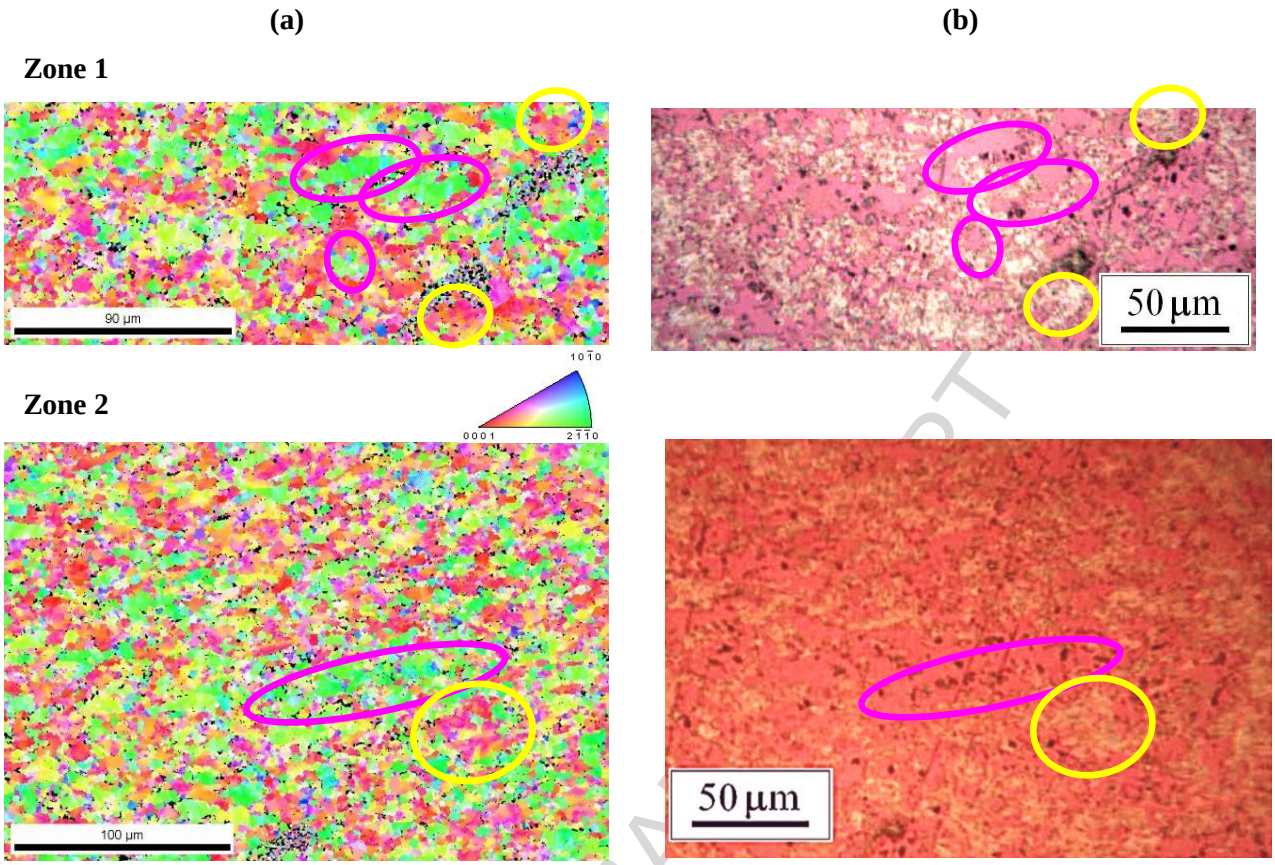

Figure 14. Comparison between: (a) IPF images of Zones 1 and 2; (b) optical micrographs of anodic coatings of Zones 1 and 2. Colored ovals indicate correspondences between characteristic regions. Yellow ovals enclose α grains oriented in the basal plane (0001), which are encoded with red to pink colors by EBSD, and the pink ovals enclose grains oriented near the $(2\bar{1}\bar{1}0)$ direction. The corresponding oxide films are yellow and pink for each grain direction, that is (0001) and $(2\bar{1}\bar{1}0)$ perpendicular to the anodized plane, respectively.

The difference in color of the oxide film is univocally related to its thickness. Vera et al. [9] reported two values of thickness of 120 and 140 nm of samples anodically oxidized in 1 M H_2SO_4 at 60 V measured by X ray reflectometry. Those values correspond to oxide films grown on grains oriented in the basal plane (0001) direction and the transversal planes $(2\bar{1}\bar{1}0)$, respectively. A thickness of 120 nm is seen in yellow color and the 140 nm is seen in pink color, in agreement with results reported in the literature [8,9] (see SI, section S3). It is then clear that the thickness of the oxides grown on basal plane is thinner than in the other directions. This is also the case of the TiG2 substrates in which there is a predominant yellow oxide due to the larger surface area of grains directed with the basal plane (0001) along the perpendicular to the anodized plane. It has been proposed [13,14] that the thickness of oxide films produced by anodic oxidation is inversely proportional to the atomic packing density in the plane exposed to oxidation. In the case of α hcp

structure, like the present case of Titanium, the plane (0001) has the highest density of $1.154a^{-2}$ where "*a*" is the hcp cell parameter. For the lateral planes the densities are $0.73a^{-2}$ for the $(2\bar{1}\bar{1}0)$ planes and $0.63a^{-2}$ for the $(10\bar{1}0)$ planes [13], showing that the thickness of the oxide films grown in the present experiments are in agreement with this proposition since the yellow oxide grows on the densest (0001) planes.

On the other hand, the pink oxide film has been determined according to the IPF to grow on transversal $(2\bar{1}\bar{1}0)$ planes, which are denser than the $(10\bar{1}0)$ planes, also in agreement with the proposed theory. It may also be concluded that the grains with pink oxides have a packing density close to $0.73a^{-2}$, corresponding to the transversal $(2\bar{1}\bar{1}0)$ plane, whereas the grains on $(10\bar{1}3)$ direction, on which also yellow oxides grow, have a packing density similar to the highest value of $1.154\ a^{-2}$. The inverse relation between the thickness of the anodic oxide and packing density has been explained on the basis of the electrochemistry of the process. The presence of a higher electron density on the surface, due to a higher packing density, reduce the rate of oxidation because of an interaction among the Ti substrate, the forming oxide and the electrolyte which affect the local electric field; thus producing less oxide with respect to less dense planes in the same period of oxidation time. In this regard, Leonardi et.al. [25] said that the growth rate of anodic TiO_2 nanotubes gradually increases with the decreasing planar atomic density of the titanium substrate, because in the thin compact oxide the electron donor concentration and electronic conductivity are higher, which leads to a competition between oxide growth and other electrochemical oxidation reactions, such as the oxygen evolution, upon anodic polarization. Hermann et al. [26] also observed influence of crystallographic orientation of Ti alloy grains on the nanotubes formation.

In summary, the TiG2 sheet has a texture consisting of 55% of the surface area in the basal plane direction or tilted less than 45º, and the remaining 45% distributed in the other transversal orientations without a preferred one since none of them represent more than 7% of the total. In the case of the TiG5 sheet, the basal direction and the less than 45º inclined direction cover 21% and the transversal $(2\bar{1}\bar{1}0)$ and $(10\bar{1}0)$ grain directions cover 18% of the total surface area. The remaining grains are elongated regions with similar directions perpendicular to the anodized plane but different than the two mentioned above, surrounded by small grains with other random directions.

The effect of orientation of the Ti grains on the coatings are as follows; in the case of TiG2 substrate the oxide coatings has a nearly homogeneously yellow color corresponding to 120 nm thickness on prevalent basal hcp orientation, with some tonalities which were not possible to correlate with precision. In the case of the TiG5 substrates, the colors of the oxides on the different

grains were pink and yellow. The pink oxides with thickness of 140 nm were observed on grains on the $(10\bar{1}0)$ and $(2\bar{1}\bar{1}0)$ directions and in between this last one and the (0001) direction, *i.e.* $(11\bar{2}4)$. The yellow oxides with a thickness of 120 nm were observed on the basal (0001) direction and between this one and the $(10\bar{1}0)$ direction, *i.e.* $(10\bar{1}3)$.

3.4. Effect of processing promoting a reduction on oxide thickness dispersion

The effect of grain orientation on the thickness of anodic oxide films have been also reported in the literature for cp Titanium [13-18]. Since for many applications a smooth coating thickness is desired, mechanisms to minimize this effect on α Ti have been proposed. The procedures have been related to physical and electrochemical aspects of the process, such as increased growth rate [13,18], oxidation time [27], stirring [28] and electrolyte temperature [28,29].

Some of these procedures have been applied in the present investigation, for obtaining uniform color-thicknesses or reducing the color-thickness difference for TiG5 alloys. The aspects we have considered are described in Tables 1 and 2, and the results were as follows.

3.4.1. Voltage increasing rate to reach 60 V

All the results presented in the previous sections were obtained using an increasing rate of 1.2 V/s until reaching 60 V, where it was fixed during 1 min. For evaluating the effect of the rate, we increased the voltage at a rate of 5.8 V/s, almost five times the previous one, following previous reports [13,18] indicating that increasing the rate from 0.0001 V/s to 0.01 V/s in the anodic oxidation of grade 2 Ti the thickness should be more homogeneous in a policrystalline substrate.

Both reports are in agreement with the results obtained in the present investigation for oxide films produced on grade 2 Ti (TiG2 plate); as observed by the homogeneous color shown in Figures 6 and 9. However, for the case of the grade 5 Ti alloy substrate (TiG5 plate) there were no significant differences on the results when the rate was increased from 1.2 V/s to 5.8 V/s, that is, when the 60 V is reached in 50 s and 10.34 s, respectively. Moreover, the overall color of the oxide is the same indicating that the initial stage of oxidation does not affect the kinetic of the process, nor the final oxide thickness for each grain orientation. This lack of effect of the voltage increase rate on TiG5 could be due to the presence of the β grains surrounding the α grains, the Al and V alloying, the grain size or the texture itself, in ways that must be analyzed from the kinetic point of view.

3.4.2. Oxidation time at 60 V

Using a rate of 5.8 V/s the oxidation time at 60 V was increased from 1 min to 15 min. The results do not show significant changes in relative thicknesses for different grain orientations. The effects of oxidation time have been reported to increase roughness [27,29] due to a gradual crystallization of the TiO_2 films on Titanium plates (99.8% Ti) [27]. However no further crystallization occurs according to XRD results shown in Figure 15, where only peaks of the substrate TiG5 (α and β) are shown and no peaks of anatase nor rutile are evident.

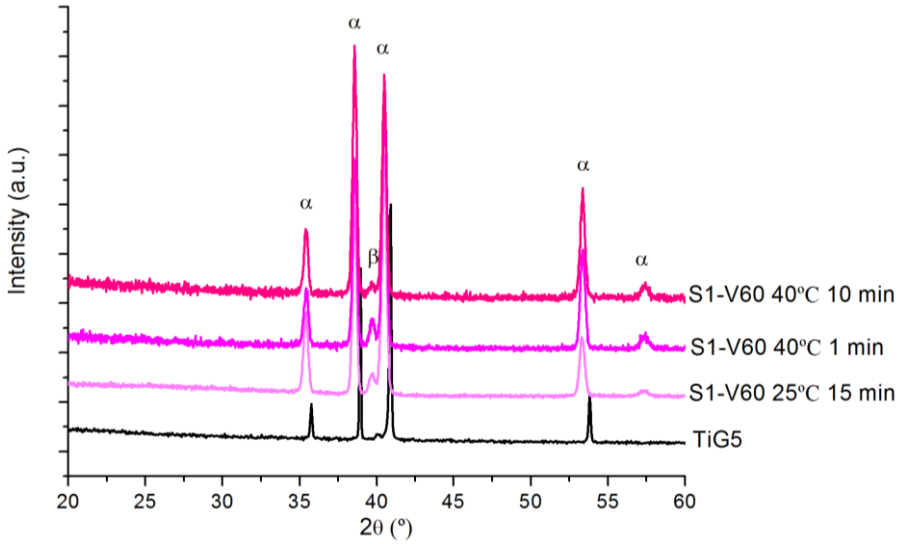

Figure 15. Normalized diffractograms of TiG5 substrate and samples oxidized at different electrolyte temperatures during different time. α and β phases are indicated.

3.4.3. Electrolyte stirring

A TiG5 plate was oxidized for 1 min with a voltage rate of 5.8 V/s with magnetic stirring of the electrolyte, following reports that stirring minimize the non-uniformity of the oxide layer on grade 5 Ti alloy [28]. The attempt was based on the assumption that the cause of non-uniformity is associated with temperature stratification at the anode-electrolyte interface, which may be prevented by stirring. However, the results obtained in the present experiments did not show any improvement in oxide thickness uniformity.

3.4.4. Temperature of the electrolyte and oxidation time at high temperature

The results obtained for an oxidation process for 1 min at 60 V, room temperature of 25 ºC, no stirring and a voltage increasing rate of 5.8 V/s were compared with those obtained by keeping the oxidation time for 1 or 10 min and elevating the temperature to 40 ºC.

The results show that increasing the temperature to 40 ºC and the oxidation time from 1 to 10 min produces oxide layers with different but non-uniform colors, as observed in Figure 16. The color is due to the formation of different thickness oxide films, obtained by oxidation with a larger current density [28] produced by larger electrolyte conductivity at higher temperature. Despite the higher temperature of the electrolyte, crystallization does not occur at 60 V according to XRD results shown in Figure 15, where only α and β peaks, and no peaks of anatase nor rutile, are shown.

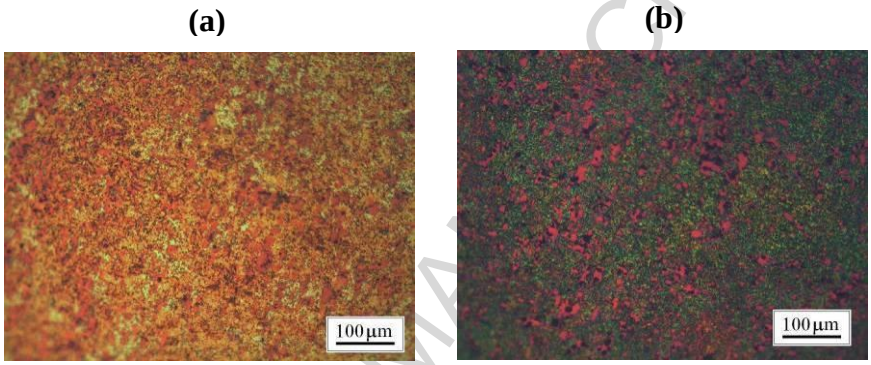

Figure 16. Optical micrographs of coatings obtained at 60 V with 1 M H_2SO_4 electrolyte at 40 °C for: (a) 1 min; (b) 10 min.

3.4.5. Heat treatments before oxidation promoting a reduction on oxide thickness dispersion

The second set of experiments performed on TiG5 substrates before oxidation, oriented to diminish the effect of texture on thickness in-homogeneity, consisted on three different heat treatments, as mentioned in Table 2.

The effect of the different heat treatments on substrate microstructure can be observed in Figure 17. Figure 17 (a) corresponds to the microstructure of a substrate before heat treatment and Figure 17 (b), (c) and (d) to the microstructure obtained after TT1, TT2 and TT3, respectively.

The structures are as the original showing from elongated grains, as in Figure 17 (a), to an equiaxial structure, as in Figure 17 (d), as time and temperature of heat treatments increase.

After heat treatments, TiG5 samples were oxidized in 1 M H_2SO_4 solution at 25 ºC, a voltage rate of 5.8 V/s, a final voltage of 60 V during 1 min and no stirring. The results of the anodic oxidation performed on the three heat-treated plates can be observed in Figure 18 (b-d). Overall, the colors of

the oxide films are more uniform in the three cases than in the oxidized original TiG5 plate (Figure 18 (a)), indicating an improvement in thickness uniformity, with a predominant pink color and less yellow color. This improvement could be associated to heat treatment recrystallization, modifying the texture of the plates [30], but already starting from a better-oriented population of crystals. Figure 19 shows the evolution of the texture of all three heat-treated samples through their IPFs. Because of increasing temperatures and heat-treating times the texture evolves to a strongly oriented <$2\bar{1}\bar{1}0$> directions //ND, reaching a value of 12 times random. Those preferred directions produce films with uniformly distributed pink color.

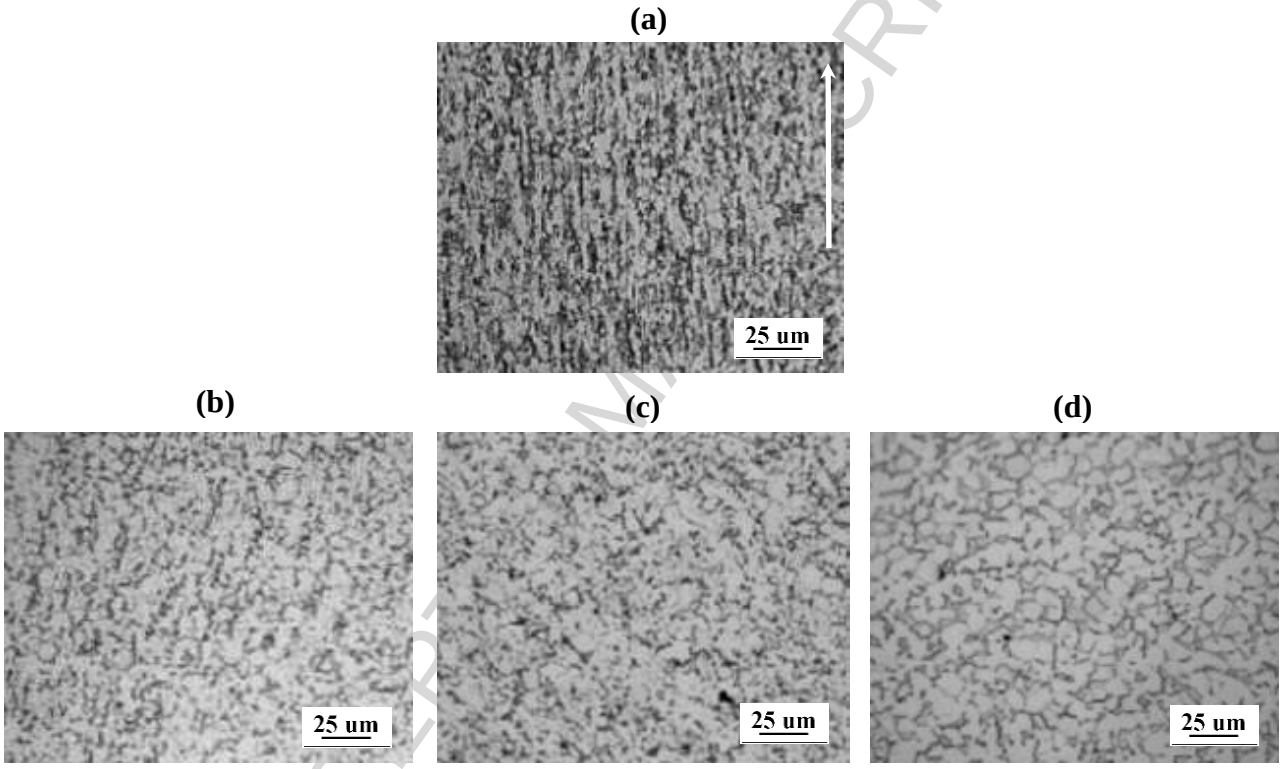

Figure 17. Optical micrographs of microstructure of original TiG5 plate (a), and TiG5 plate with different heat treatments: (b) TT1; (c) TT2; (d) TT3.

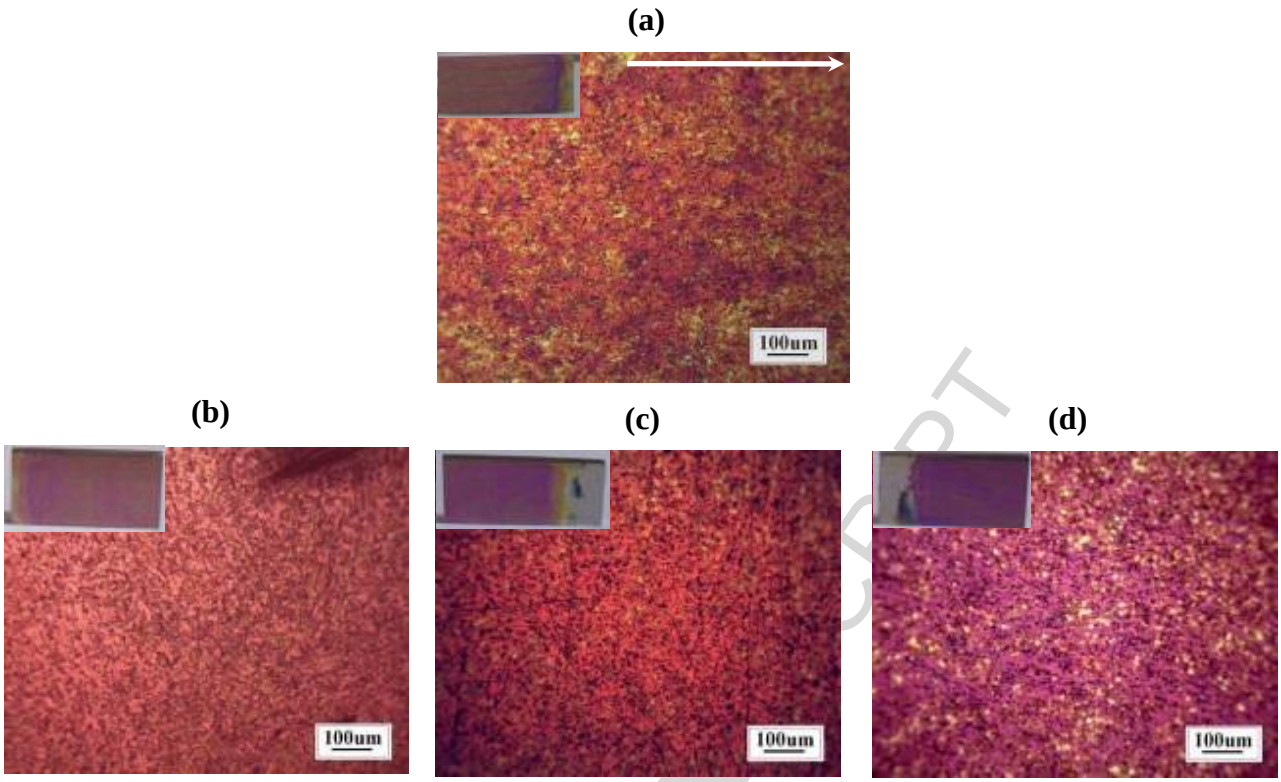

Figure 18. Macrographs (top left corner) and optical micrographs of 60 V anodic coatings of original TiG5 plate (a) and TiG5 plate with different heat treatments: (b) TT1; (c) TT2; (d) TT3.

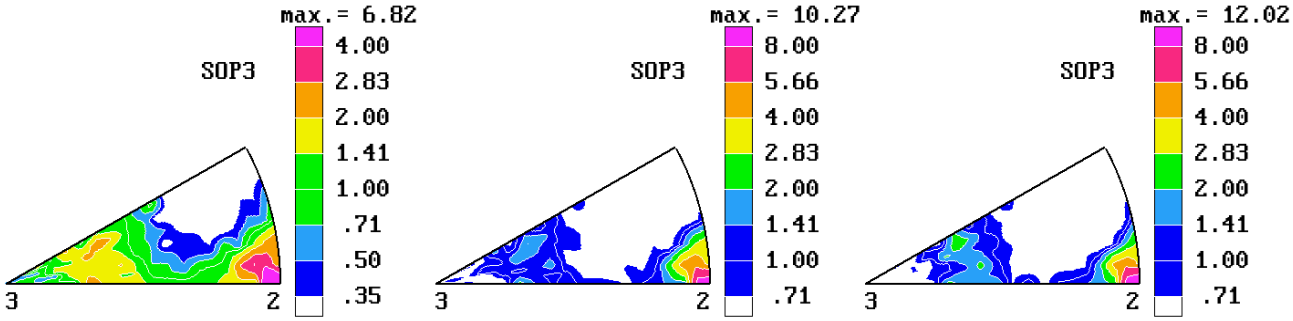

Figure 19. ND Inverse Pole Figures for TiG5 plates with increasing temperatures and heat treatment times: (a) TT1; (b) TT2; (c) TT3.

4. Conclusions

The effect of substrate textures on colors and tonalities of TiO_2 coatings on Ti alloys obtained by anodic oxidation were investigated. The substrates were Ti grade 2 and 5 alloys, from different origins and processes.

Anodic oxidation was performed in a 1 M H_2SO_4 solution at 60 V during 1 min. Before oxidation, the substrates were analyzed by EBSD to determine the crystalline orientations of the surface

substrate grains. After oxidation, the color distributions were correlated with the crystalline orientations.

The colors of the oxides vary depending on the alloy type and on the crystal direction perpendicular to the anodized surface, because of the induced thicknesses, as previously known from the literature. In the case of TiG5 substrates, two colors (yellow and pink) predominate, which correspond to thickness of 120 and 140 nm, respectively. Each coating thickness corresponds to substrate grain orientations in the basal and transversal directions, respectively. The effect is related to the atomic density of the exposed grain surfaces, which slows oxidation rate at higher densities producing a thinner film than in less dense exposed surfaces.

In order to reduce the effect, several anodic oxidation process parameters were investigated. It is concluded that changes in oxidation parameters has no or little effect on producing more homogeneous coating thicknesses. However, pre-oxidation heat treatment of the substrate, which may modify the texture of the surface, resulted in less inhomogeneous thickness of anodic coatings.

So far, the best strategy for obtaining homogeneous thickness oxide layers seems to be the choice, through an adequate thermomechanical processing, of proper textures. Our particular rolled TiG5 plate subject to further heat treatments provided a strongly oriented population of $[2\bar{1}\bar{1}0]$ planes contained in the rolling plane and a consequent uniform color.

Acknowledgements

The authors wish to thank the financial support of CONICET and ANPCyT, to Diego Lamas from CITEDEF for XRD measurements and Biol. Vanina Tartalini and Eng. Pablo Risso for careful preparation of samples and EBSD maps measurements.

References

[1] N.G. Bardina: Anodic oxide films, Russian Chemical Reviews, 33 (5) (1964) 286-295.

[2] A. Aladjem: Anodic oxidation of titanium and its alloys, Journal of Materials Science, 8 (5) (1973) 688-704.

[3] M.V. Diamanti, M.P. Pedeferri: Effect of anodic oxidation parameters on the titanium oxides formation, Corrosion Science, 49 (2) (2007) 939‑948.

[4] N.K. Kuromoto, R.A. Simao, G.A. Soares: Titanium oxide films produced on commercially pure titanium by anodic oxidation with different voltages, Materials Characterization, 58 (2) (2007) 114‑121.

[5] X. Chen, S.S. Mao: Titanium dioxide nanomaterials: synthesis, properties, modifications, and applications, 107 (2007) 2891-2959.

[6] M.V. Diamanti, B. Del Curto, M.P. Pedeferri: Anodic oxidation of titanium: from technical aspects to biomedical applications, Journal of Applied Biomaterials & Biomechanics, 9 (1) (2011) 55-69.

[7] E. Gaul: Coloring titanium and related metals by electrochemical oxidation, Journal of Chemical Education, 70 (1993) 176-178.

[8] M.L. Vera, M.A. Alterach, M.R. Rosenberger, D.G. Lamas, C.E. Schvezov, A.E. Ares: Characterization of TiO_2 Nanofilms Obtained by Sol-gel and Anodic Oxidation, Nanomaterials and Nanotechnology, 4 (10) (2014) 1-11.

[9] M.L. Vera: Obtención y Caracterización de Películas Hemocompatibles de TiO_2, Ph. D. Thesis, Instituto Sabato, UNSAM – CNEA. IS/TD –71/13, Buenos Aires, (2013).

[10] M.L. Vera, A.E. Ares, M.R. Rosenberger, D.G. Lamas y C.E. Schvezov: Determinación por reflectometría de rayos X del espesor de recubrimientos de TiO_2 obtenidos por oxidación anódica, Anales AFA, 21 (2009) 174-178.

[11] M.L. Vera, M.R. Rosenberger, C.E. Schvezov, A.E. Ares: Fabrication of TiO_2 crystalline coatings by combining anodic oxidation and heat treatments. International Journal of Biomaterials, 2015 (2015), 1- 9.

[12] M.V. Diamanti, B. Del Curto, M.P. Pedeferri: Interference colors of thin oxide layers on titanium, 33 (3) (2008), 221-228.

[13] S. Kudelka, A. Michaelis, J.W. Schultze: Effect of texture and formation rate on ionic and electronic properties of passive layers on Ti single crystals; Electrochimica Acta, 41 (1996) 863-870.

[14] M.V. Diamanti, M.P. Pedeferri, C.A. Schuh: Thickness of anodic titanium oxides as a function of crystallographic orientation of the substrate; Metallurgical and Materials Transactions A, 39 (2008) 2143-2147.

[15] E. Matykina, R. Arrabal, P. Skeldon, G.E. Thompson, H. Habazaki: Influence of grain orientation on oxygen generation in anodic titania; Thin Solid Films, 516 (2008) 2296-2305.

[16] S. Kudelka, J.W. Schultze: Photoelectrochemical imaging and microscopic reactivity of oxidized Ti; Electrochimica Acta, 42 (18) (1997) 2817-2825.

[17] A. Michaelis, J.W. Schultze: Anisotropy micro-ellipsometry for in-situ determination of optical and crystallographic properties of anisotropic solids and layers with Ti/TiO_2 as an example; Thin Solid Films, 274 (1996) 82-94.

[18] M.R. Kozlowski, P.S. Tyler, W.H. Smyrl, R.T. Atanasoski: Photoelectrochemical microscopy of oxide films on metals: Ti/TiO_2 interface; Surface Science, 194 (1988) 505-530.

[19] Norma ASTM B 367 – 93 Standard Specification for Titanium and Titanium Alloy Castings (2004).

[20] J.S. Kallend, U.F. Kocks, A.D. Rollett, H.-R. Wenk: Operational texture analysis; Materials Science and Engineering A, 132 (1991) 1-11.

[21] S.-H. Choi, D.H. Kim, H.W. Lee, B.S. Seong, K. Piao, R.Wagoner: Evolution of the deformation texture and yield locus shape in an AZ31 Mg alloy sheet under uniaxial loading; Materials Science and Engineering A, 526 (2009) 38-49.

[22] C. Leyens, M. Peters: Titanium and Titanium Alloys; Fundamentals and Applications, 1ª ed., WILEY-VCH, Köln, 2003.

[23] M.R. Bache, W.J. Evans: Impact of texture on mechanical properties in an advanced titanium alloy; Materials Science and Engineering A, 319-321 (2001) 409-414.

[24] G. Lütjering, J.C. Williams: Titanium, Springer, 2003.

[25] S. Leonardi, V. Russo, A. Li Bassi, F. Di Fonzo, T.M. Murray, H. Efstathiadis, A. Agnoli, J. Kunze-Liebhäuser: TiO_2 Nanotubes: Interdependence of substrate grain orientation and growth rate; American

Chemical Society - Applied Materials and Interfaces, 7 (3) (2015) 1662-1668.

[26] R. Hermann, M. Uhlemann, H. Wendrock, G. Gerbeth, B. Buchner: Magnetic field controlled single crystal growth and surface modification of titanium alloys exposed for biocompatibility; Journal of Crystal Growth, 318 (2011) 1048-1052.

[27] S.K. Poznyak, D.V. Talapin, A.I. Kulak: Electrochemical oxidation of titanium by pulsed discharge in electrolyte; Journal of Electroanalytical Chemistry; 579 (2005) 299-310.

[28] A. K. Sharma: Anodizing titanium for space applications; Thin Solid Films, 208 (1992) 48-54.

[29] D. Capek, M.-P. Gigandet, M. Masmoudi, M. Wery, O. Banakh: Long-time anodization of titanium in sulphuric acid; Surface & Coatings Technology, 202 (2008) 1379-1384.

[30] Liu-Qing Yang, Yan-Qing Yang: Deformed microstructure and texture of Ti6Al4V alloy; Transactions of Nonferrous Metals Society of China, 24 (2014) 3103-3110.

Highlights

- Influence of texture of the Titanium substrates on anodic coatings were analysed.
- On different Ti substrate grain orientations grew different coatings thickness.
- Oxide color depends on the Ti alloy and the crystal grain orientation.
- The texture effect on the color coatings is more evident on laminated substrates.
- Substrate heat treatments resulted in less inhomogeneous coatings thickness.